Shell structure at $N = 28$ near the dripline: Spectroscopy of ^{42}Si, ^{43}P, and ^{44}S

J. Fridmann,[1] I. Wiedenhöver,[1] A. Gade,[2] L. T. Baby,[1] D. Bazin,[2] B. A. Brown,[2] C. M. Campbell,[2] J. M. Cook,[2] P. D. Cottle,[1] E. Diffenderfer,[1] D.-C. Dinca,[2] T. Glasmacher,[2] P. G. Hansen,[2] K. W. Kemper,[1] J. L. Lecouey,[2] W. F. Mueller,[2] E. Rodriguez-Vieitez,[3] J. R. Terry,[2] J. A. Tostevin,[4] K. Yoneda,[2] and H. Zwahlen[2]

[1]*Department of Physics, Florida State University, Tallahassee, Florida 32306-4350, USA*

[2]*National Superconducting Cyclotron Laboratory and Department of Physics and Astronomy, Michigan State University, East Lansing, Michigan 48824-1321, USA*

[3]*Nuclear Science Division, Lawrence Berkeley National Laboratory, Berkeley, California 94720, USA*

[4]*Department of Physics, School of Electronics and Physical Sciences, University of Surrey, Guildford, Surrey GU2 7XH, United Kingdom*

(Received 27 February 2006; published 13 September 2006)

Measurements of the $N = 28$ isotones ^{42}Si, ^{43}P, and ^{44}S using one- and two-proton knockout reactions from the radioactive beam nuclei ^{44}S and ^{46}Ar are reported. The knockout reaction cross sections for populating ^{42}Si and ^{43}P and a 184 keV γ-ray observed in ^{43}P establish that the $d_{3/2}$ and $s_{1/2}$ proton orbits are nearly degenerate in these nuclei and that there is a substantial $Z = 14$ subshell closure separating these two orbits from the $d_{5/2}$ orbit. The increase in the inclusive two-proton knockout cross section from ^{42}Si to ^{44}S demonstrates the importance of the availability of valence protons for determining the cross section. New calculations of the two-proton knockout reactions that include diffractive effects are presented. In addition, it is proposed that a search for the $d_{5/2}$ proton strength in ^{43}P via a higher statistics one-proton knockout experiment could help determine the size of the $Z = 14$ closure.

DOI: 10.1103/PhysRevC.74.034313 PACS number(s): 21.10.Pc, 21.60.Cs, 25.70.Hi, 27.40.+z

I. INTRODUCTION

The quest for information about shell structure in $N = 28$ nuclei near the neutron dripline is of central importance to the field of nuclear structure physics for two reasons. First, the nuclei in the vicinity of ^{42}Si provide the first arena in which ideas about how changes in the spin-orbit force affect shell structure near the neutron dripline can be tested. The $N = 28$ shell closure is the lightest neutron shell closure caused by the spin-orbit force, which is responsible for all shell closures in heavier nuclei. At present, the $N = 28$ shell closure is the only major neutron shell closure driven by the spin-orbit force that is experimentally accessible. It has been predicted that the spin-orbit force affecting the neutron orbits weakens close to the neutron dripline both because of the weak binding of neutrons in this vicinity and the role of the continuum [1,2]. Indeed, it has been predicted [3–9] that the $N = 28$ shell closure should be less well developed, or even collapse altogether, in the nuclei near ^{42}Si. Three recent experimental results, one a measurement of the lifetime of the β-decay of ^{42}Si [10], the second the determination that ^{43}Si is bound [11] and the third a mass measurement of ^{42}Si [12] have been used to argue that the $N = 28$ shell closure has narrowed or collapsed in ^{42}Si, resulting in a well-deformed shape for this nucleus. On the other hand, it has been argued in Refs. [13,14] that a possible proton subshell closure at $Z = 14$ would have a strong effect on the structure of ^{42}Si, preventing it from being well-deformed.

The second reason that experiments on nuclei near ^{42}Si are important is that they are providing a rigorous testing regime for experimental techniques that will be used heavily at the next generation of radioactive beam facilities, including the Rare Isotope Accelerator. Among these techniques are the intermediate-energy knockout reactions in which cross sections provide spectroscopic information similar to that obtained for many years from direct transfer reactions used at low-energy stable beam facilities [15,16].

In the present article, we provide a comprehensive report of a set of measurements of the $N = 28$ isotones ^{42}Si, ^{43}P, and ^{44}S using one- and two-proton knockout reactions from the radioactive beam nuclei ^{44}S and ^{46}Ar. A brief account of this work was given in Ref. [17]. In addition to more detail regarding the results in Ref. [17], this article also reports: new calculations of the two-proton knockout reactions that include diffractive contributions that were not available prior to the publication of Ref. [17]; new shell model calculations that allow us to refine the conclusions we draw from the two-proton knockout results regarding the nature of the $Z = 14$ shell closure; and calculations of the expected distribution of $d_{5/2}$ proton hole strength in the one-proton knockout reaction spectrum of ^{43}P.

Section II of this article will include details of the experimental techniques and results. Section III will discuss the experimental results on ^{42}Si and ^{44}S and the theoretical calculations on two-proton knockout reactions. In Sec. IV, we discuss the experimental and theoretical results regarding ^{43}P. Section V will provide a brief summary.

II. EXPERIMENTAL DETAILS

The present experiments were performed at the National Superconducting Cyclotron Laboratory at Michigan State University using the Coupled Cyclotrons Facility (CCF). Beams of the radioactive nuclei ^{44}S and ^{46}Ar were produced via fragmentation of a primary beam of 140 MeV/nucleon ^{48}Ca provided by the CCF. The primary beam was fragmented on a 705 mg/cm^2 thick beryllium target, and the fragmentation

products were separated in the A1900 fragment separator [18]. The separator selected secondary beams of 98.6 MeV/nucleon ^{44}S and 98.1 MeV/nucleon ^{46}Ar. The ^{44}S secondary beam had a momentum spread of $\pm 1.0\%$ and a purity of 75%; the rate of ^{44}S particles impinging on the secondary target averaged 400 particles/s. For the ^{46}Ar secondary beam, the momentum spread was $\pm 0.5\%$ and the purity was 95%; the beam rate on the secondary target was 24×10^4 ^{46}Ar particles/s. Both the ^{44}S and ^{46}Ar secondary beam particles were identified event-by-event by their time-of-flight before impinging on the secondary target.

The knockout reactions were induced on a secondary beryllium target of thickness 375 mg/cm^2. The residual projectile-like nuclei were detected in the S800 spectrograph [19]. Gamma-rays emitted at the secondary target location were detected using the SeGA array of segmented high purity germanium detectors [20] in coincidence with the residues in the S800 spectrograph.

The measurement of the residual nucleus ^{42}Si was performed via the two-proton knockout reaction on the ^{44}S secondary beam, ^{9}Be(^{44}S,^{42}Si)X. The integrated secondary beam was 1.14×10^8 ^{44}S particles. The ^{43}P measurement was performed with the one-proton knockout reaction on the ^{44}S secondary beam, ^{9}Be(^{44}S,^{43}P)X; the integrated secondary beam for this measurement was 1.1×10^7 ^{44}S particles. Finally, ^{44}S was measured via the two-proton knockout reaction on the ^{46}Ar secondary beam, ^{9}Be(^{46}Ar,^{44}S)X with an integrated secondary beam of 7.3×10^9 ^{46}Ar particles.

The spectra from the S800 used to identify residual nuclei are shown in Fig. 1. The vertical axes correspond to the energy loss in the ion chamber at the focal plane of the S800, while the horizontal axis plots the path-corrected time of flight between the object point of the spectrograph and the focal plane. The inclusive cross sections for production of the ^{42}Si, ^{43}P and ^{44}S residual nuclei were 0.12(2) mb, 7.6(11) mb and 0.23(2) mb, respectively. The momentum distributions for these residual nuclei were within the acceptance of the S800 spectrograph for the respective reactions and S800 settings.

The γ-ray spectra in coincidence with the ^{42}Si, ^{43}P and ^{44}S residual nuclei are shown in Fig. 2. These spectra are Doppler-reconstructed so that they appear as in the rest frames of the residual nuclei. The total photopeak efficiency of the SeGA array for this experiment was 5.7% at 180 keV, 2.2% at 1 MeV, and 1.3% at 2 MeV.

There are no discernible γ-ray peaks in the ^{42}Si spectrum.

The ^{43}P spectrum includes a single large peak at 184(3) keV. No other peaks are clearly discernable, although there are background counts up to 1 MeV.

For ^{44}S, the $2_1^+ \rightarrow 0_{gs}^+$ γ-ray previously reported in Refs. [21–23] is seen clearly in our spectrum and we assign an energy of 1.329(10) MeV. This γ-ray was first observed in the Coulomb excitation study of Glasmacher *et al.* [21], where an energy of 1.297(18) MeV was given. More recently, Sohler *et al.*, in a report of their study of ^{44}S via the fragmentation of ^{48}Ca [22], gave an energy of 1.350(10) MeV for this transition. Finally, the report of the observation of an isomer in ^{44}S in Ref. [23] is accompanied by the report of an energy of 1.329 MeV for the $2_1^+ \rightarrow 0_{g.s.}^+$ transition, with no experimental uncertainty given. It is likely there are other γ-rays in the spectrum below 1.2 MeV, but the resolving power of the present experiment does not allow us to distinguish them clearly.

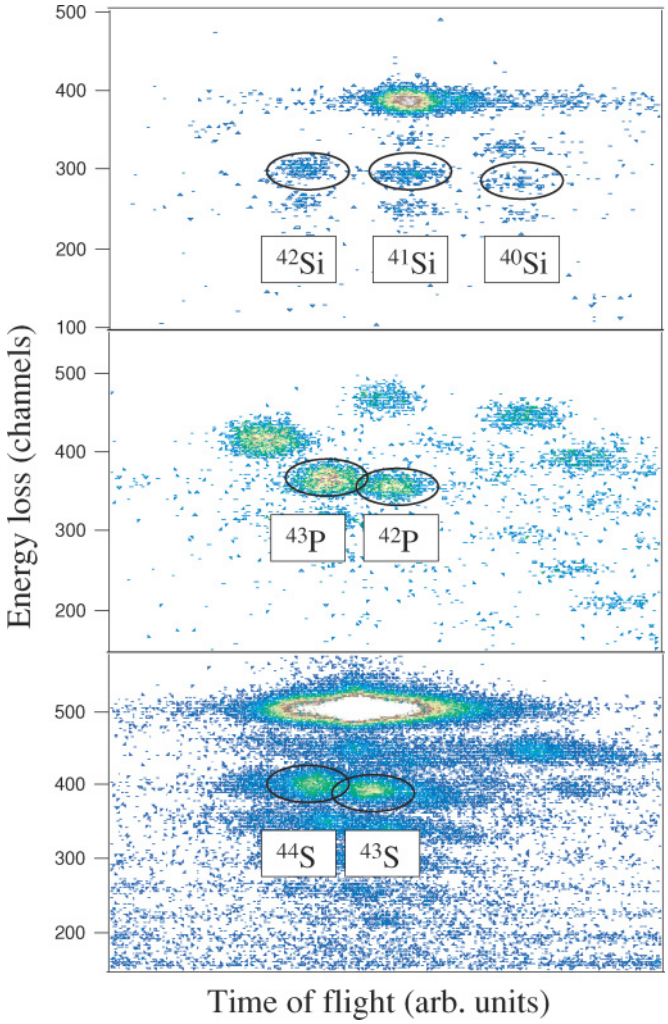

FIG. 1. (Color online) Particle spectra used to identify ^{42}Si from the two-proton knockout reaction from ^{44}S (top), ^{43}P from the one-proton knockout reaction from ^{44}S (middle), and ^{44}S from the two-proton knockout reaction from ^{46}Ar (bottom). The energy loss in the ion chamber at the focal plane of the S800 spectrograph is plotted on the vertical axis, and the horizontal axis plots the path-corrected time of flight between the object point of the spectrograph and the focal plane, with shorter flight times to the right.

III. ^{42}SI AND ^{44}S

A. Shell structure

The present measurement of ^{42}Si provided two experimental conclusions: first, that the inclusive cross section for producing this nucleus in the two-proton knockout reaction is 0.12(2) mb, and second, that there are no discernible γ-rays in the spectrum.

The inclusive cross section is small, smaller than any previously observed for the two-proton knockout reaction [16]. Bazin *et al.* [16] pointed out that the cross section for the

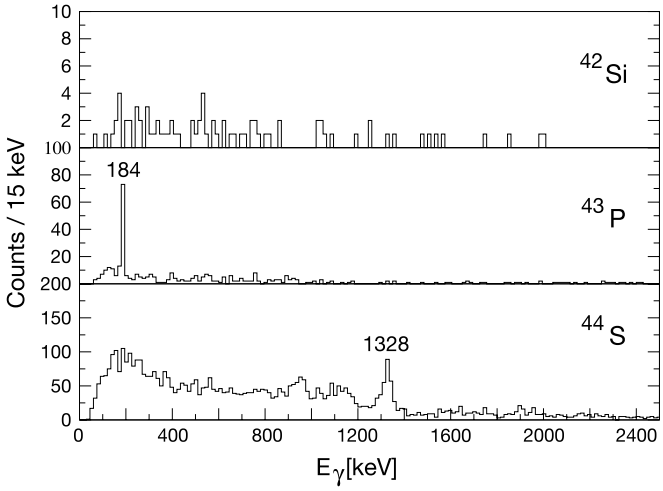

FIG. 2. Spectra of γ-rays detected in coincidence with ^{42}Si (top panel), ^{43}P (middle), and ^{44}S (bottom) in the ^{44}S(^{9}Be,^{42}Si)X, ^{44}S(^{9}Be,^{43}P)X, and ^{46}Ar(^{9}Be,^{44}S)X reactions, respectively.

two-proton knockout reaction depends on the number of valence protons, so the small cross section observed here suggests that a shell closure occurs at $Z = 14$ where the $d_{5/2}$ proton orbit fills. Indeed, in the $N = 28$ isotone ^{48}Ca, the $(d,^{3}\mathrm{He})$ reaction [24,25] revealed a large gap between the $d_{5/2}$ proton orbit and the $d_{3/2}$ and $s_{1/2}$ proton orbits (which are nearly degenerate in ^{48}Ca). The small two-proton knockout cross section provides strong evidence that the $Z = 14$ shell gap is substantial in ^{42}Si as well.

We have performed shell model calculations and reaction calculations to examine how neutron and proton shell structure affect the spectroscopy of ^{42}Si and ^{44}S. The shell model calculations use the interaction of Ref. [26] with the neutrons occupying a model space including the $0f_{7/2}$ and $1p_{3/2}$ orbits and the protons occupying the full *sd* space. The two-nucleon amplitudes that resulted were used to calculate two-proton knockout cross sections with a model that extends that described in Ref. [17] by including diffractive effects.

B. Two-proton removal calculations

The two-proton removal reaction from an intermediate energy neutron-rich projectile nucleus has recently been shown to proceed as a sudden, direct reaction process [16,27]. While the associated two-proton structures and the reaction mechanism were treated only approximately in Ref. [16], a far more complete calculational scheme has since been detailed in Ref. [27]. This dealt with that part of the two-nucleon removal cross section arising from the stripping (inelastic breakup) mechanism and the theoretical approach combined fully the two-nucleon shell-model configurations and their associated spectroscopic amplitudes with eikonal direct reaction theory. This analysis provided further evidence for the direct nature of the reaction mechanism in such systems. The theoretical calculations of the two-proton-removal cross sections presented here follow the formalism developed in Ref. [27]. In addition, we include a full calculation of the cross section contributions from the mechanism in which one proton is absorbed (stripped) while a second is elastically dissociated (diffracted) by the target. An estimate of the (smaller) cross section due to the removal of both nucleons by the elastic dissociation (diffraction) mechanism is also included, as is outlined below.

The two knocked-out nucleons are assumed to be removed from a set of active, partially occupied single-particle orbitals ϕ_j with spherical quantum numbers $n(\ell j)m$. The shell model wave function of the removed nucleons in the projectile ground state, relative to any given residue (or core) state f, is the sum over the contributing two-particle configurations,

$$\Psi^{(f)}_{J_i M_i}(1,2) = \sum_{I\mu\alpha} C_\alpha^{J_i J_f I}(I\mu J_f M_f | J_i M_i)[\overline{\phi_{j_1} \otimes \phi_{j_2}}]_{I\mu}. \quad (1)$$

Here α denotes these available configurations (j_1, j_2) and $[\overline{\phi_{j_1} \otimes \phi_{j_2}}]$ is their normalized, antisymmetrized wave function [27]. The $C_\alpha^{J_i J_f I}$ are the signed two-nucleon spectroscopic amplitudes which are calculated here using the shell model code OXBASH [28].

The model used for the two-nucleon stripping cross section was discussed fully in Ref. [27], to which the reader is referred. The partial cross section to a residue final state f is the integral over all projectile center-of-mass (c.m.) impact parameters b and average over the two-removed-nucleon wave functions

$$\sigma_{\mathrm{str}} = \frac{1}{(2J_i+1)} \sum_{M_i} \int d\boldsymbol{b} |\mathcal{S}_c|^2 \langle \Psi^{(f)}_{J_i M_i} | (1 - |\mathcal{S}_1|^2) \times (1 - |\mathcal{S}_2|^2) | \Psi^{(f)}_{J_i M_i} \rangle, \quad (2)$$

where the $\mathcal{S}_i$ are the eikonal S-matrices [29] for the elastic scattering of the two nucleons (1,2) and the A-body core with the target. These are functions of their impact parameters and are assumed to be spin-independent. This cross section expression accounts for those events in which the residue emerges from the reaction having missed or interacted only elastically with the target, as described by $|\mathcal{S}_c|^2$, and two nucleons are removed through inelastic collisions with the target. This inelasticity and the associated removal of flux from the nucleon-target elastic channels is described by the product of the nucleon-target absorption probabilities $(1 - |\mathcal{S}_i|^2)$.

Additional contributions to the knockout cross section, when one nucleon, say 1, is removed in an elastic interaction with the target while the second nucleon is absorbed, enter the eikonal model expression for the absorption cross section via the term

$$\sigma_1 = \frac{1}{2J_i+1} \sum_{M_i} \int d\boldsymbol{b} |\mathcal{S}_c|^2 \langle \Psi^{(f)}_{J_i M_i} | |\mathcal{S}_1|^2 (1 - |\mathcal{S}_2|^2) | \Psi^{(f)}_{J_i M_i} \rangle, \quad (3)$$

and similarly for nucleon 2. These diffraction-plus-absorption terms require further attention since the cross section in Eq. (3) includes processes in which nucleon 1 remains bound to the residue. These correspond to a single nucleon absorption from the projectile populating bound states of an $(A+1)$-body residue. Such effects could be ignored in an analogous discussion of the nuclear breakup of Borromean nuclei, such as ^{11}Li [30], where there are no two-body bound (valence) states of the core and the (nonabsorbed) neutron.

These single-nucleon stripping contributions are removed by projecting off bound nucleon-residue final states, by replacing

$$|\mathcal{S}_1|^2 \rightarrow \mathcal{S}_1^* \left[1 - \sum_{j''m''} \left|\phi_{j''}^{m''}\right\rangle \left\langle\phi_{j''}^{m''}\right| \right] \mathcal{S}_1, \qquad (4)$$

in Eq. (3). Here the notation implies a summation over the bound eigenstates $n(\ell'' j'')m''$ of nucleon 1 and the core and we have used the (..| and |..) bra-kets to denote integration over the coordinates of this single nucleon. In the calculations presented we include all the active single particle orbitals in this sum. We find that the $\sigma_1 + \sigma_2$ contribution to the cross section is similar to $\sigma_{\rm str}$.

Finally, we include an estimate of the (smaller) cross section due to the removal of both (tightly-bound) nucleons by elastic dissociation. Our estimate makes use of the reduction in the cross section when a single nucleon is elastically dissociated compared to it being stripped, $\sigma_i/\sigma_{\rm str}$. We thus estimate the two-nucleon elastic breakup cross section to be $\sigma_{\rm diff} \approx [\sigma_i/\sigma_{\rm str}]^2\sigma_{\rm str}$. Since, for the cases discussed here, and more generally, $\sigma_i/\sigma_{\rm str} \approx 0.35$–$0.4$, then $\sigma_{\rm diff}$ makes a contribution of order 6–8% to the two-proton removal partial cross sections. The theoretical two-proton removal cross sections presented are the sum of these contributions, i.e. $\sigma_{\rm th} = \sigma_{\rm str} + \sigma_1 + \sigma_2 + \sigma_{\rm diff}$.

The S-matrices in Eq. (2) were calculated from the core and target one-body matter densities using the optical limit of Glauber's multiple scattering theory [29,31]. A Gaussian nucleon-nucleon (NN) effective interaction was assumed [32] with a range of 0.5 fm. This calculates residue- and nucleon-target S-matrices and corresponding reaction cross sections in line with measurements in the 50–100 MeV/nucleon energy range, e.g., [33]. The strength of the interaction was determined, in the usual way [34], by the free pp and np cross sections and the real-to-imaginary ratios of the forward NN scattering amplitudes, α_{pp} and α_{np}. The latter affect the calculation of the diffractive contributions but are of no consequence for the stripping terms, that require only $|\mathcal{S}_i|^2$. For the ^{9}Be(^{46}Ar,^{44}S)X and ^{9}Be(^{44}S,^{42}Si)X reaction calculations the density of ^{9}Be was assumed to be of Gaussian form with a root mean squared (rms) matter radius of 2.36 fm [35]. The densities of the core nuclei, ^{44}S and ^{42}Si, were taken from spherical, Skyrme (SkX interaction) Hartree-Fock calculations [36]. These have rms matter radii of 3.45 fm and 3.44 fm, respectively.

Our calculations suppose that the removed protons occupy the $0d_{5/2}$, $0d_{3/2}$ and $1s_{1/2}$ sd-shell orbitals. The nucleon single-particle wave functions were calculated in a Woods-Saxon potential well with the conventional radius and diffuseness parameters $r_0 = 1.25$ fm and $a = 0.70$ fm. The strengths of the binding potentials were adjusted to support bound eigenstates with half the physical ground-state to ground-state two-proton separation energies. These two-proton separation energies were taken as $S_{2p} = 33.42$ MeV and 40.46 MeV for ^{46}Ar and ^{44}S. Also, due to these large separation energies, we did not included the small corrections to the nucleon separation energies for transitions to bound, excited final states.

Full details of the formalism for these new diffractive terms, and their application to several (test-case) *sd*-shell nuclei, with better-understood structures, will be presented elsewhere [37]. Using the full *sd*-shell model spectroscopy, the calculated inclusive cross sections consistently overpredict the measured cross sections by a factor of two, requiring a corresponding suppression, $R_s(2N) \approx 0.5$, of the two-nucleon shell model strengths. The analogous suppression effects in nucleus-induced [15,38] and electron-induced [39] single-nucleon knockout reactions are now well documented, and are of order $R_s(1N) \approx 0.6$ for a wide range of nuclei with (N, Z) asymmetries and/or separation energies similar to those of the present study.

C. Discussion

The calculated inclusive two-proton knockout cross section for ^{42}Si, using wavefunctions generated with the shell-model effective interaction of Ref. [26], is 0.32 mb, about a factor of three larger than the experimental value of 0.12(2) mb. However, taking into account the expected $R_s(2N)$ value of order 0.5, discussed above, there is a closer agreement with the measured value. It is also worth noting that 92% of the cross section calculated for ^{42}Si using these parameters is located in the ground state; therefore, the contribution of the excited states to the inclusive cross section measurement is likely to be small.

As mentioned above, the reason that the cross section is small is because of the $Z = 14$ shell gap; that is, the energy gap between the $d_{3/2}$-$s_{1/2}$ pair and the $d_{5/2}$ orbit is large. We can examine how the theoretical cross section depends on the size of the $Z = 14$ gap by performing several calculations in which the gap is reduced. The Ref. [26] parametrization sets the $d_{3/2}$-$d_{5/2}$ gap as 5.9 MeV. There is an experimental reason to believe that this gap may be too large—an analysis of the centroids of proton hole strength observed in ^{47}K via the ^{48}Ca(d,^{3}He) reaction and reported in Ref. [25] gives a $d_{3/2}$-$d_{5/2}$ gap of 4.8 MeV.

More calculations were performed in which this gap was reduced by 1 MeV and 3 MeV. In addition, the size of the $N = 28$ neutron gap was also reduced by 1 MeV (from its value of 3.6 MeV for ^{42}Si) to examine how this affects the cross section. In all, four calculations were performed—the first with both the proton and neutron gaps at the values from Ref. [26]; the second with the neutron gap reduced by 1 MeV and the proton gap left at the value from Ref. [26]; the third with both the proton and neutron gaps reduced by 1 MeV from the Ref. [26] values; and the fourth with the neutron gap reduced by 1 MeV from the Ref. [26] value and the proton gap reduced by 3 MeV from the Ref. [26] value.

The cross section results from the four calculations, including the $R_s(2N) = 0.5$ suppression, are shown in the top panel of Fig. 3. The reduction of the neutron gap does not affect the two-proton knockout cross section. Furthermore, the reduction of the proton gap by 1 MeV does not significantly affect the cross section, either. This is not surprising since even with this reduction the gap is 4.9 MeV. However, a 3 MeV reduction in the proton gap does result in a significant increase in the cross section.

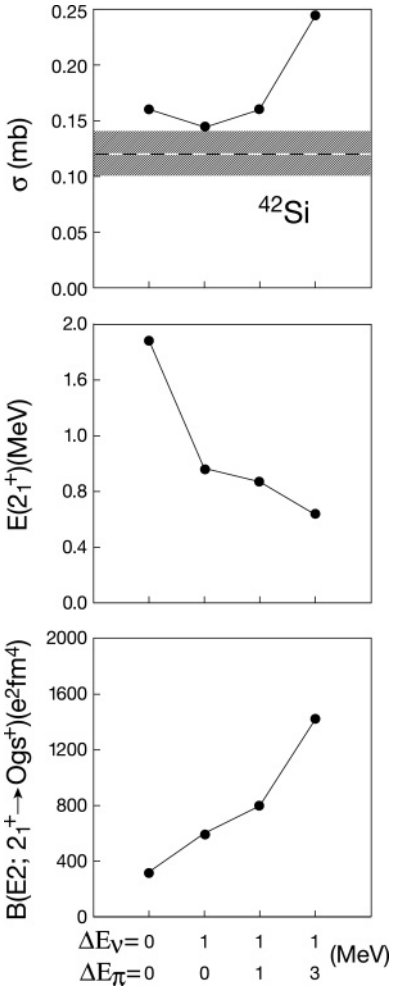

FIG. 3. Spectroscopic observables in ^{42}Si calculated with the shell model and four sets of parameters for the $Z = 14$ and $N = 28$ (sub)shell closures, as described in the text. The four sets of parameters are denoted by $\Delta E_\nu = 0$, $\Delta E_\pi = 0$ (shell gaps used in Ref. [26]), $\Delta E_\nu = 1$, $\Delta E_\pi = 0$ (neutron shell gap reduced by 1 MeV from the Ref. [26] value), $\Delta E_\nu = 1$, $\Delta E_\pi = 1$ (both neutron and proton shell gaps reduced by 1 MeV from the Ref. [26] values), and $\Delta E_\nu = 1$, $\Delta E_\pi = 3$ (neutron gap reduced by 1 MeV and proton gap reduced by 3 MeV from Ref. [26] values). The top panel is the inclusive cross section for the two-proton knockout reaction from ^{44}S (with the present experimental result shown as the dashed line and the experimental uncertainty cross-hatched). The middle panel is the energy of the 2_1^+ state, and the bottom panel is the reduced electromagnetic matrix element $B(E2; 2_1^+ \rightarrow 0_{\text{g.s.}}^+)$.

The bottom two panels of Fig. 3 show two other sets of spectroscopic results for ^{42}Si from the four shell model calculations—the energy of the lowest 2_1^+ state, $E(2_1^+)$, and the reduced electromagnetic matrix element connecting the 2_1^+ state to the ground state, $B(E2; 2_1^+ \rightarrow 0_{\text{g.s.}}^+)$. Of these two observables, the reduced matrix element is the more reliable indicator of quadrupole collectivity. Reducing the neutron gap by 1 MeV has a strong effect on both these observables. Adding the 1 MeV reduction of the proton gap has little additional effect on $E(2_1^+)$, but causes a significant additional increase in $B(E2; 2_1^+ \rightarrow 0_{\text{g.s.}}^+)$. The large (3 MeV) reduction in the proton gap from its original value of 5.9 MeV causes a near-doubling in the $B(E2; 2_1^+ \rightarrow 0_{\text{g.s.}}^+)$ matrix element from its value with a 1 MeV proton gap reduction. At this point, proton excitations are playing a large role in driving deformation.

A calculation of the inclusive two-proton knockout cross section for ^{44}S using shell model wavefunctions determined with the parameters of Ref. [26] yields a result of 0.66 mb, which is (as in the case of ^{42}Si) much larger than the experimental value of 0.23(2) mb. Once again, the $R_s(2N)$ systematics lead to an expected theoretical value of around 0.33 mb, in closer agreement with the measured value. The calculation qualitatively reproduces the increase in cross section from ^{42}Si to ^{44}S with the addition of valence protons.

It is reasonable to conclude from comparing the cross section data to these calculations that there is a large gap at $Z = 14$, although these data cannot provide a quantitative measure of the size of this gap. With respect to the urgent question of whether the $N = 28$ gap has narrowed from its size in ^{48}Ca or even disappeared altogether, the present data cannot provide any insights. Instead, a measurement of $B(E2; 2_1^+ \rightarrow 0_{\text{g.s.}}^+)$ in ^{42}Si would provide much more information on the size of the neutron gap and, therefore, the strength of the orbital spitting between $l = 1$ and $l = 3$ and spin-orbit interaction on neutron orbits near the neutron dripline.

IV. ^{43}P

The one-proton knockout reaction preferentially populates states that have the structure of a proton hole in the beam nucleus [15]. Therefore, the states in ^{43}P populated with the largest cross sections in the one-proton knockout reaction on ^{44}S are expected to be those that are single protons in the $d_{3/2}$ or $s_{1/2}$ orbits, or a single $d_{5/2}$ proton hole. In ^{47}K, (a proton hole coupled to the doubly-magic nucleus ^{48}Ca), the centroids of the strength from the $d_{3/2}$ and $s_{1/2}$ proton orbits are seen to be separated by only 300 keV [24,25]. In the present measurement of ^{43}P, the 184 keV γ-ray suggests that the strength of one of these two single-proton orbits is concentrated in the ground state with the strength of the other orbit concentrated in an excited state at 184 keV. The $d_{5/2}$ strength is expected at higher excitation energies in ^{43}P, as discussed below.

The cross sections for the ground state and 184 keV state are large and therefore support this picture. The inclusive cross section—which includes both the ground state and the 184 keV state—is 7.6(11) mb. An examination of the residue-γ-ray coincidences shows that the 184 keV state accounts for 75±15% of the cross section. The combination of this observation regarding the relative cross sections of the two states and calculations based on the prescription given in Refs. [29,40] provide a strong argument that the $s_{1/2}$ proton strength is concentrated in the ground state, while the $d_{3/2}$ strength is concentrated in the 184 keV state. A shell model calculation similar to that described in Sec. III using the Ref. [26] parameters (including the 5.8 MeV $d_{3/2} - d_{5/2}$ proton orbit splitting), yields a cross section of 3.7 mb for a ground state that consumes 98% of the $s_{1/2}$ strength, while a state that consumes 99% of the $d_{3/2}$ strength is located at 0.20 MeV and has a cross section of 7.9 mb. The experimental and theoretical

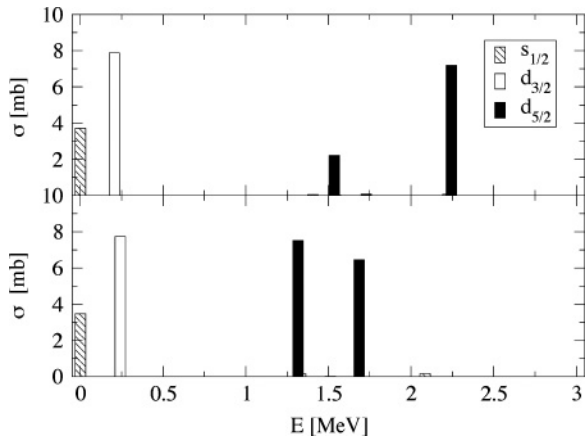

FIG. 4. Distribution of the strength for the $s_{1/2}$, $d_{3/2}$ and $d_{5/2}$ proton strength in ^{43}P from the one-proton knockout reaction on ^{44}S calculated using two different values for the $d_{3/2} - d_{5/2}$ proton spacing and (otherwise) the parameters from Ref. [26]. The top panel uses the spacing from Ref. [26], while the bottom panel uses a spacing 1 MeV smaller.

inclusive cross sections are thus in the ratio $R_s = 0.66(9)$, consistent with systematics of suppression factors from other well-bound-nucleon knockout studies [15,40]. The excited state fraction from theory, 68%, is also in good agreement with the measured value of 75(15)%. If the $d_{3/2} - d_{5/2}$ proton orbit splitting is reduced by 1 MeV (to reflect the experimental result in ^{47}K as discussed in Sec. III), then the ground state holds 95% of the $s_{1/2}$ strength and has a cross section of 3.5 mb, with 98% of the $d_{3/2}$ strength residing in a state at 0.24 MeV that has a 7.7 mb cross section. These two calculations are consistent with each other in that they predict that the $d_{3/2}$ state has a cross section a little more than twice the $s_{1/2}$ cross section, which is approximately what is seen in the data.

As demonstrated in Sec. III, the spin-orbit splitting of the $d_{3/2}$ and $d_{5/2}$ proton orbits is an important parameter for interpreting the results of the present two-proton knockout study of ^{42}Si, other measurements of this nucleus and data on nearby nuclei. While no evidence for $d_{5/2}$ strength was observed in the present data set, the one-proton knockout reaction on ^{44}S provides a means for determining the $d_{3/2} - d_{5/2}$ proton spin-orbit splitting. A calculation of the distribution of $d_{5/2}$ proton hole strength in ^{43}P using the Ref. [26] parameters, including the 5.8 MeV $d_{3/2} - d_{5/2}$ splitting and the resulting cross sections for population of these states in the one proton knockout reaction (with the cross section calculation prescription as described in Refs. [29,40]) is shown in the top panel of Fig. 4. It provides a prediction of a concentration of $d_{5/2}$ proton hole strength (7.2 mb of cross section) at 2.24 MeV (although it is quite likely this strength is fragmented over several states—explaining its apparent absence from the spectrum of Fig. 2), with a somewhat smaller concentration (2.2 mb) at 1.54 MeV. This yields a centroid of 2.1 MeV. If instead the $d_{3/2} - d_{5/2}$ splitting is set to 4.8 MeV, as shown in the bottom panel of Fig. 4, the centroid of the $d_{5/2}$ strength is 1.5 MeV (with a 6.4 mb concentration at 1.67 MeV and a 7.4 mb concentration at 1.32 MeV). We conclude that the location of the $d_{5/2}$ proton hole strength in the one-proton knockout reaction provides a sensitive scale for determining the $d_{3/2} - d_{5/2}$ proton spin-orbit splitting, and that this provides a motivation for another ^{44}S one-proton knockout experiment with the sensitivity (increased by means of greater statistics) required to detect the fragments of the $d_{5/2}$ strength.

V. SUMMARY

The present data on the $N = 28$ isotones ^{42}Si, ^{43}P and ^{44}S provide important insights regarding the most important factors influencing nuclear structure in this vicinity. First of all, the knockout reaction cross sections for populating ^{42}Si and ^{43}P and the 184 keV γ-ray observed in ^{43}P firmly establish that the $d_{3/2}$ and $s_{1/2}$ proton orbits are nearly degenerate in these nuclei and that there is a substantial $Z = 14$ subshell closure separating these two orbits from the $d_{5/2}$. The increase in the inclusive two-proton knockout cross section from ^{42}Si to ^{44}S demonstrates the importance of the availability of valence protons for determining the cross section. In addition, a search for the $d_{5/2}$ proton strength in ^{43}P via a higher statistics one-proton knockout experiment could quantify the size of the $Z = 14$ closure.

ACKNOWLEDGMENTS

This work was supported by the National Science Foundation through grants PHY-0456463, PHY-0110253, PHY-0244453 account 61-2275 (7032), the Department of Energy through grant DE-FG02-02ER-41220, the State of Florida, and by the United Kingdom Engineering and Physical Sciences Research Council (EPSRC) Grant No. EP/D003628.

[1] W. Nazarewicz and R. F. Casten, Nucl. Phys. **A682**, 295c (2001).
[2] D. Warner, Nature (London) **430**, 517 (2004).
[3] T. R. Werner *et al.*, Phys. Lett. **B333**, 303 (1994).
[4] T. R. Werner *et al.*, Nucl. Phys. **A597**, 327 (1996).
[5] J. Terasaki, H. Flocard, P.-H. Heenan, and P. Bonche, Nucl. Phys. **A621**, 706 (1997).
[6] G. A. Lalazissis, A. R. Farhan, and M. M. Sharma, Nucl. Phys. **A628**, 221 (1998).
[7] G. A. Lalazissis, D. Vretenar, P. Ring, M. Stoitsov, and L. M. Robledo, Phys. Rev. C **60**, 014310 (1999).
[8] S. Peru, M. Girod, and J. F. Berger, Eur. Phys. J. A **9**, 35 (2000).
[9] R. Rodriguez-Guzman, J. L. Egido, and L. M. Robledo, Phys. Rev. C **65**, 024304 (2002).
[10] S. Grevy *et al.*, Phys. Lett. **B594**, 252 (2004).
[11] M. Notani *et al.*, Phys. Lett. **B542**, 49 (2002).
[12] H. Savajols *et al.*, Eur. Phys. J. A **25**, s01, 23 (2005).
[13] P. D. Cottle and K. W. Kemper, Phys. Rev. C **58**, 3761 (1998).
[14] E. Caurier, F. Nowacki, and A. Poves, Nucl. Phys. **A742**, 14 (2004).
[15] P. G. Hansen and J. A. Tostevin, Annu. Rev. Nucl. Part. Sci. **53**, 219 (2003).

[16] D. Bazin *et al*., Phys. Rev. Lett. **91**, 012501 (2003).
[17] J. Fridmann *et al*., Nature **435**, 922 (2005).
[18] D. J. Morrissey *et al*., Nucl. Instrum. Methods Phys. Res. B **204**, 90 (2003).
[19] D. Bazin *et al*., Nucl. Instrum. Methods Phys. Res. B **204**, 629 (2003).
[20] W. F. Mueller *et al*., Nucl. Instrum. Methods Phys. Res. A **466**, 492 (2001).
[21] T. Glasmacher *et al*., Phys. Lett. **B395**, 163 (1997).
[22] D. Sohler *et al*., Phys. Rev. C **66**, 054302 (2002).
[23] S. Grevy *et al*., Eur. Phys. J. A **25**, 111 (2005).
[24] P. Doll *et al*., Nucl. Phys. **A263**, 210 (1976).
[25] S. M. Banks *et al*., Nucl. Phys. **A437**, 381 (1985).
[26] S. Nummela *et al*., Phys. Rev. C **63**, 044316 (2001).
[27] J. A. Tostevin, G. Podolyák, B. A. Brown, and P. G. Hansen, Phys. Rev. C **70**, 064602 (2004).
[28] The computer code OXBASH, B. A. Brown *et al*., MSU-NSCL Report Number 524.
[29] J. A. Tostevin, Nucl. Phys. **A682**, 320c (2001).
[30] G. F. Bertsch, K. Hencken, and H. Esbensen, Phys. Rev. C **57**, 1366 (1998).
[31] R. J. Glauber, in *Lectures in Theoretical Physics*, edited by W. E. Brittin (Interscience, New York, 1959), Vol. 1, p. 315.
[32] J. A. Tostevin, J. Phys. G **25**, 735 (1999).
[33] S. Kox *et al*., Phys. Rev. C **35**, 1678 (1987).
[34] L. Ray, Phys. Rev. C **20**, 1857 (1979).
[35] A. Ozawa *et al*., Nucl. Phys. **A691**, 599 (2001).
[36] B. A. Brown, Phys. Rev. C **58**, 220 (1998).
[37] J. A. Tostevin *et al*. (to be published).
[38] A. Gade *et al*., Phys. Rev. Lett. **93**, 042501 (2004).
[39] G. J. Kramer, H. P. Blok, and L. Lapikás, Nucl. Phys. **A679**, 267 (2001), and references therein.
[40] A. Gade *et al*., Phys. Rev. C **69**, 034311 (2004).